ORIGINAL ARTICLE

Assessing IGS GPS/Galileo/BDS-2/BDS-3 phase bias products with PRIDE PPP-AR

Jianghui Geng[*] , Songfeng Yang and Jiang Guo

Abstract

Ambiguity Resolution in Precise Point Positioning (PPP-AR) is important to achieving high-precision positioning in wide areas. The International GNSS (Global Navigation Satellite System) Service (IGS) and some other academic organizations have begun to provide phase bias products to enable PPP-AR, such as the integer-clock like products by Centre National d'Etudes Spatials (CNES), Wuhan University (WUM) and the Center for Orbit Determination in Europe (CODE), as well as the Uncalibrated Phase Delay (UPD) products by School of Geodesy and Geomatics (SGG). To evaluate these disparate products, we carry out Global Positioning System (GPS)/Galileo Navigation Satellite System (Galileo) and BeiDou Navigation Satellite System (BDS-only) PPP-AR using 30 days of data in 2019. In general, over 70% and 80% of GPS and Galileo ambiguity residuals after wide-lane phase bias corrections fall in ± 0.1 cycles, in contrast to less than 50% for BeiDou Navigation Satellite (Regional) System (BDS-2); moreover, around 90% of GPS/Galileo narrow-lane ambiguity residuals are within ± 0.1 cycles, while the percentage drops to about 55% in the case of BDS products. GPS/Galileo daily PPP-AR can usually achieve a positioning precision of 2, 2 and 6 mm for the east, north and up components, respectively, for all phase bias products except those based on German Research Centre for Geosciences (GBM) rapid satellite orbits and clocks. Due to the insufficient number of BDS satellites during 2019, the BDS phase bias products perform worse than the GPS/Galileo products in terms of ambiguity fixing rates and daily positioning precisions. BDS-2 daily positions can only reach a precision of about 10 mm in the horizontal and 20 mm in the vertical components, which can be slightly improved after PPP-AR. However, for the year of 2020, BDS-2/BDS-3 (BDS-3 Navigation Satellite System) PPP-AR achieves about 50% better precisions for all three coordinate components.

Keywords: Precise point positioning, Phase bias products, Ambiguity resolution, Multi-GNSS

Introduction

As a high-precision positioning technique which is independent of nearby reference stations, Global Navigation Satellite System (GNSS) Precise Point Positioning (PPP) has been applied widely to achieve millimeter-level static positioning (Zumberge et al., 1997). However, the positioning precision of PPP is rather limited since undifferenced ambiguities cannot be estimated as integers directly (cf. Gabor & Nerem, 1999; Geng et al., 2009; Ghoddousi-Fard & Dare, 2006; Tétreault et al., 2005).

In the past decade, a few approaches have been proposed to achieve PPP Ambiguity Resolution (PPP-AR).

Ge et al. (2008) computed receiver- and satellite-dependent Uncalibrated Phase Delays (UPD) and then fixed single-receiver ambiguities to their integer candidates successfully. Wide-lane UPDs were estimated as a constant over 24 h using the Melbourne–Wübbena (MW) combination observations (Melbourne, 1985; Wübbena, 1985). Narrow-lane UPDs were estimated over shorter intervals, e.g.,15 min. While the UPD method used the International GNSS Service (IGS) legacy clock products, Laurichesse et al. (2009) and Collins et al. (2010) formulated "integer clocks" by absorbing narrow-lane UPDs into the legacy satellite clocks. To mitigate possible biases introduced into pseudorange after applying the integer clocks, Laurichesse et al. (2009) aligned the integer clocks with the legacy clocks to an offset of smaller than half

---

*Correspondence: jgeng@whu.edu.cn
GNSS Research Center, Wuhan University, Wuhan, China

Geng *et al. Satell Navig*　　(2021) 2:17

Page 2 of 15

of the narrow-lane wavelength, and Collins et al. (2010) estimated a second clock product dedicated to pseudorange. Alternatively, Geng et al. (2019a) developed a modified phase clock/bias model where phase clocks were computed with narrow-lane UPDs deducted from integer clocks in advance. In this study, we call all UPDs, integer clocks and phase clock/biases as "phase bias products" for simplicity.

Based on the methods above, there have been several organizations providing phase bias products. Centre National d'Etudes Spatials (CNES) has been releasing Global Positioning System (GPS) integer clock products since 2011 (Laurichesse, 2011). GPS/Galileo (Galileo Navigation Satellite System) products were also provided after 2015. Besides, CNES provides multi-GNSS phase bias products based on GFZ (GeoForschungsZentrum) rapid orbits and clocks. In 2019, the School of Geodesy and Geomatics at Wuhan University (SGG) started to provide GPS/Galileo/BDS-2 (BeiDou Navigation Satellite (Regional) System)/QZSS (Quasi-Zenith Satellite System) UPD products. They calculated three types of products with respect to the precise orbits and clocks provided by GFZ, CNES and CODE (Center for Orbit Determination in Europe) (Hu et al., 2020). Different from the UPD and integer clock products, Wuhan University (WHU) has been releasing GPS/Galileo/BDS-2/BDS-3(BeiDou-3 Navigation Satellite System) phase clock/bias products (Geng et al., 2019a). Their GPS only and multi-GNSS products have spanned the past 15 and 4 years, respectively. Similarly, CODE has issued GPS/Galileo phase bias products since 2019 (Schaer et al., 2018).

Since there have been many phase bias products estimated by different academic organizations, in this study, we aim at making a detailed assessment on their quality and analyzing the PPP-AR performance. This study is organized as follows: Section 2 derives the PPP-AR models for UPDs, integer clocks and phase bias/clocks. Section 3 shows the strategies of data processing. Section 4 displays the stability and precision of these phase bias products as well as the PPP-AR solutions. Finally, Section 5 draws the conclusions.

Methods
GNSS observational functions
We start with the raw GNSS observation equations,

$$
\begin{cases}
P_{r,m}^s = \rho_{r,m}^s + c(t_r - t^s) + \mu_m I_r^s + b_{r,m} - b_m^s + \varepsilon_{r,m}^s \\
L_{r,m}^s = \rho_{r,m}^s + c(t_r - t^s) - \mu_m I_r^s + \lambda_m N_{r,m}^s + B_{r,m} - B_m^s + e_{r,m}^s
\end{cases}
\tag{1}
$$

where r and s denote the receiver and satellite, respectively; m refers to the signal frequency and $m = 1, 2$; $P_{r,m}^s$ and $L_{r,m}^s$ denote the pseudorange and carrier-phase measurements, respectively; $\rho_{r,m}^s$ denotes the geometric distance including slant troposphere delay and antenna phase center errors; c denotes the speed of light in vacuum; t_r and t^s represents the receiver and satellite clock errors, respectively; I_r^s denotes the slant ionospheric delay while μ_m is the coefficient related to signal frequencies; λ_m denotes the wavelength; $N_{r,m}^s$ denotes the integer ambiguity; $b_{r,m}$ and $B_{r,m}$ denotes the receiver hardware biases on pseudorange and carrier-phase, respectively, while b_m^s and B_m^s denotes the satellite hardware biases; $\varepsilon_{r,m}^s$ and $e_{r,m}^s$ denotes the pseudorange and carrier-phase noise, respectively.

In order to eliminate the first-order ionospheric delay, the ionosphere-free combination observable is formed, which can be formulated as

$$
\begin{cases}
|P_{r,\mathrm{IF}}^s = \rho_r^s + c(t_r - t^s) + b_{r,\mathrm{IF}} - b_{\mathrm{IF}}^s + \varepsilon_{r,\mathrm{IF}}^s \\
|L_{r,\mathrm{IF}}^s = \rho_r^s + c(t_r - t^s) + \lambda_1 N_{r,\mathrm{IF}}^s + B_{r,\mathrm{IF}} - B_{\mathrm{IF}}^s + e_{r,\mathrm{IF}}^s
\end{cases}
\tag{2}
$$

where "IF" denotes Ionosphere-Free combination.

Then, to fix wide-lane ambiguities, the Melbourne-Wübbena combination observable (Melbourne, 1985; Wübbena, 1985) is used,

$$
N_{r,w}^s = \lambda_w \left(\frac{L_{r,1}^s + z_{r,1}^s}{\lambda_1} - \frac{L_{r,2}^s + z_{r,2}^s}{\lambda_2} \right) \\
- \frac{f_1 \left(P_{r,1}^s + z_{r,1}^s \right) + f_2 \left(P_{r,2}^s + z_{r,2}^s \right)}{f_1 + f_2}
\tag{3}
$$

where $N_{r,w}^s$ denotes the wide-lane ambiguity and λ_w denotes the wide-lane wavelength; f denotes the signal frequency. Of particular note, $z_{r,1}^s$ and $z_{r,2}^s$ denote the antenna phase center corrections which are

$$
\begin{cases}
z_{r,1}^s = z_{r,1} \sin \theta_r^s + z_1^s \\
z_{r,2}^s = z_{r,2} \sin \theta_r^s + z_2^s
\end{cases}
\tag{4}
$$

where $z_{r,1}$ and $z_{r,2}$ are the vertical phase center offsets of the receiver antenna on frequencies 1 and 2; similarly, z_1^s and z_2^s are those for the satellite antenna; θ_r^s denotes the elevation angle of satellite s with respect to receiver r. We note that the antenna phase center corrections in Eq. (4) on the Melbourne-Wübbena combination is exceptionally important to the Galileo satellites since their phase center errors differ among frequencies.

To remove receiver-related biases, single-difference ambiguities are always formed before calculating satellite phase biases and performing PPP-AR. Wide-lane

Geng *et al. Satell Navig*   (2021) 2:17

Page 3 of 15

ambiguities are easier to be fixed due to their long wavelength of several tens of centimeters. Afterwards, using the corresponding float ambiguities $N_{r,\text{IF}}^s$ and the fixed wide-lane ambiguities $\overline{N_{r,w}^s}$, narrow-lane ambiguities $N_{r,n}^s$ can be written as

$$N_{r,n}^s = \frac{f_1 + f_2}{f_1} N_{r,\text{IF}}^s - \frac{f_2}{f_1 - f_2} \overline{N_{r,w}^s} \qquad (5)$$

UPD based PPP-AR

Based on the IGS legacy clocks, the observation functions applying UPD products can be formulated as (Ge et al., 2008)

$$\begin{cases} |\Delta P_{r,\text{IF}}^{i,j} + c\Delta t_U^{i,j} = \Delta \rho_r^{i,j} + \varepsilon_{r,\text{IF}}^{i,j} \\ |\Delta L_{r,\text{IF}}^{i,j} + c\Delta t_U^{i,j} - \frac{f_2^2}{f_1^2 - f_2^2}\lambda_2 \overline{\Delta N_{r,w}^{i,j}} + \widetilde{\Delta B_{\text{IF}}^{i,j}} = \Delta \rho_r^{i,j} + \lambda_n \Delta N_{r,1}^{i,j} + e_{r,\text{IF}}^{i,j} \end{cases} \qquad (6)$$

where Δ denotes single difference between satellites i and j; $t_U^{i,j}$ denotes IGS legacy clock product; $\overline{\Delta N_{r,w}^{i,j}}$ is the fixed wide-lane ambiguity and $\widetilde{\Delta B_{\text{IF}}^{i,j}}$ is the narrow-lane phase bias product; $N_{r,1}^{i,j}$ is the narrow-lane ambiguity which can be resolved directly.

Integer clock based PPP-AR

For the integer clock method, narrow-lane phase biases are absorbed into satellite clocks (Collins et al., 2010; Laurichesse et al., 2009). For PPP-AR based on integer clocks, we have

$$\begin{cases} |\Delta P_{r,\text{IF}}^{i,j} + c\Delta t_I^{i,j} = \Delta \rho_r^{i,j} - \Delta b_{\text{IF}}^{i,j} + \Delta B_{\text{IF}}^{i,j} + \varepsilon_{r,\text{IF}}^{i,j} \\ |\Delta L_{r,\text{IF}}^{i,j} + c\Delta t_I^{i,j} - \frac{f_2^2}{f_1^2 - f_2^2}\lambda_2 \overline{\Delta N_{r,w}^{i,j}} = \Delta \rho_r^{i,j} + \lambda_n \Delta N_{r,1}^{i,j} + e_{r,\text{IF}}^{i,j} \end{cases} \qquad (7)$$

where $t_I^{i,j}$ denotes integer clocks. Note that $\Delta b_{\text{IF}}^{i,j}$ and $\Delta B_{\text{IF}}^{i,j}$ are not estimated and presumed to be absorbed into pseudorange residuals (Geng et al., 2019a). Collins et al., (2010) therefore chose to estimate a second satellite clock dedicated to pseudorange to absorb $\Delta b_{\text{IF}}^{i,j}$ and $\Delta B_{\text{IF}}^{i,j}$.

Phase clock/bias based PPP-AR

Similar to UPD based PPP-AR, the observation equation based on phase clocks/biases can be written as

$$\begin{cases} |\Delta P_{r,\text{IF}}^{i,j} + c\Delta t_P^{i,j} = \Delta \rho_r^{i,j} + \varepsilon_{r,\text{IF}}^{i,j} \\ |\Delta L_{r,\text{IF}}^{i,j} + c\Delta t_P^{i,j} - \frac{f_2^2}{f_1^2 - f_2^2}\lambda_2 \overline{\Delta N_{r,w}^{i,j}} + \widetilde{\Delta B_{\text{IF}}^{i,j}} = \Delta \rho_r^{i,j} + \lambda_n \Delta N_{r,1}^{i,j} + e_{r,\text{IF}}^{i,j} \end{cases} \qquad (8)$$
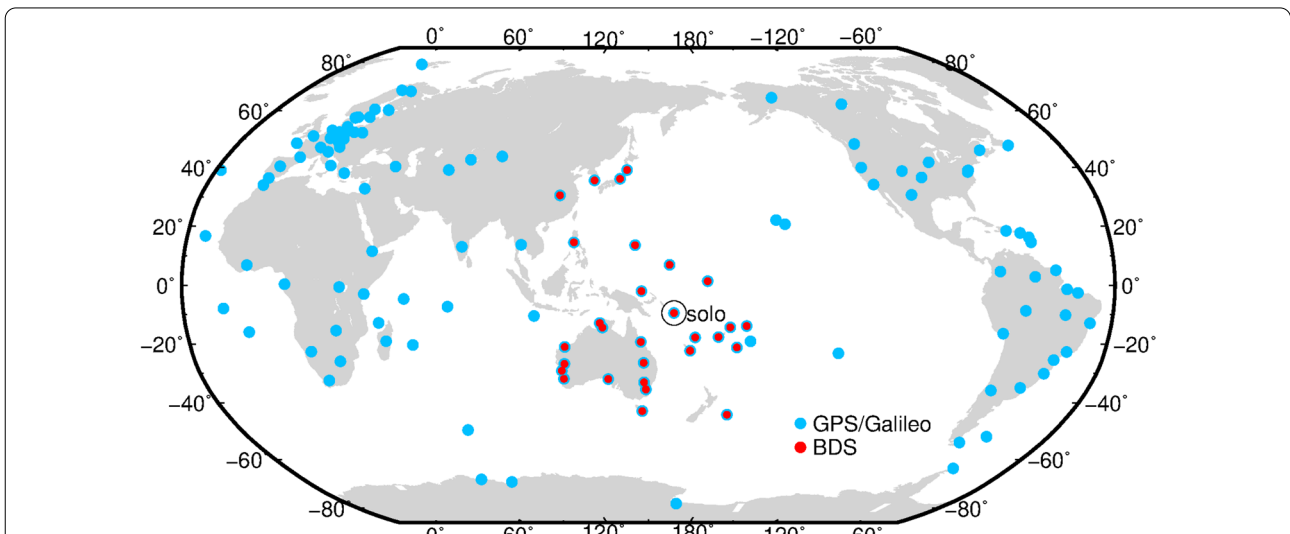
Fig. 1 Distribution of about 300 IGS stations for PPP-AR test. The blue dots denote stations for GPS/Galileo PPP-AR while the red dots denote those of BDS PPP-AR

Geng *et al. Satell Navig*   (2021) 2:17

Page 4 of 15

Table 1 Data processing strategies of PRIDE PPP-AR

Items	Strategies
Priori noise	Pseudorange: 0.3 m Carrier-phase: 0.006 cycles
Cutoff elevation	7°
Weighting strategy	Weight = 1, if elevation > 30° Weight = 4 $\sin(\text{elevation})^2$, if elevation < 30°
Antenna phase centers	igs14.atx/M14.atx/ESA BDS-2 estimations
Tidal displacements	Corrected (Petit & Luzum, 2010)
Relativistic effect	Corrected
Receiver clocks	One for each GNSS as a white-noise like parameter
Troposphere delays	Saastamoinen model (Saastamoinen, 1972) and estimated every hour using the Global Mapping Function (GMF) (Boehm et al., 2006)
Horizontal troposphere gradients	Estimated every 12 h
Ionosphere delays	First-order delays eliminated in the ionosphere-free combination and higher-order delays corrected with CODE global ionosphere maps (Fritsche et al., 2005)
Sequential bias fixing	Applied to daily and kinematic PPP with 24 h of data (Dong & Bock, 1989)
LAMBDA	Applied to hourly solutions with a ratio threshold of 3.0 (Teunissen, 1995)

where $t_P^{i,j}$ denotes the phase clocks and $\widetilde{\Delta B_{\text{IF}}^{i,j}}$ is the daily narrow-lane UPD. Note that the phase clocks have been aligned to IGS legacy satellite clocks by removing $\widetilde{\Delta B_{\text{IF}}^{i,j}}$ from the integer clocks. As a result, the phase clocks are consistent with pseudorange measurements.

Data processing

Figure 1 shows about 300 globally distributed IGS stations for the PPP-AR tests. The data processing strategies are shown in Table 1. For brevity, the phase bias products provided by WHU, CNES, CODE are termed as "WUM", "GRG" and "COM", respectively; GRG UPD products based on GFZ rapid orbit/clock products are termed as "GRG-gbm"; the UPD products of SGG based on precise orbits/clocks of GFZ, CODE and CNES are denoted as "SGG-gbm", "SGG-com" and "SGG-grg", respectively. To achieve the best PPP-AR performance, the phase bias products together with their corresponding satellite orbits, clocks, Earth rotation parameters, differential code biases and antenna corrections (Hofmann-Wellenhof et al., 2001; Kouba & Héroux, 2001) are used in PRIDE PPP-AR, as shown in Table 2 (Geng et al., 2019b). We also use the same pseudorange and carrier-phase observables prescribed by each phase bias product. Note that ambiguity-float PPP solutions are computed with phase bias corrected observations. The station positions in the IGS weekly solutions are used to benchmark the position Root Mean Square (RMS) errors of this study.

It is worth noting that the SGG and GRG phase bias products are provided in self-defined formats, while GRG-gbm, COM and WUM products are formatted

according to the standard Bias-SINEX (Software INdependent EXchange) format V1.00 (Schaer, 2016). In this study, we first convert all phase bias products into the Bias-SINEX format to fit the PRIDE PPP-AR software (Banville et al., 2020; Geng et al., 2019b). Moreover, the COM and GRG phase bias products are estimated along with satellite orbits and clocks; in contrast, the WUM products are computed along with the satellite clocks (i.e., phase clocks), while fixing the WUM orbits by Guo et al. (2015); all remaining products in Table 2 are generated by fixing third-party satellite orbits and clocks. Note that COM products correspond to the antenna phase center correction file M14.atx (ftp://ftp.aiub.unibe.ch/CODE_MGEX/CODE/), differing from igs14.atx. SGG-com and SGG-gbm use the BDS-2 satellite antenna phase center estimates provided by Dilssner et al. (2014). Galileo/BDS receiver antenna phase centers are presumed to be the same as those for GPS. Only WUM has BDS-3 phase bias products, and COM, GRG and SGG-grg do not have BDS-2 products. WUM BDS-2 phase bias products are based on B1I/B3I signals while all others are based on B1I/B2I signals.

In addition, the GRG-gbm products are computed using uncombined GNSS observations, rather than the conventional Melbourne-Wübbena and ionosphere-free combination observations (Laurichesse, 2015). The resultant wide-lane phase bias products are subject to the antenna phase center corrections. Therefore, whenever the GRG-gbm phase biases are used to fix Melbourne-Wübbena wide-lane ambiguities, Eq. (4) has to be applied, especially for the Galileo satellites of which the antenna phase center errors differ distinctively among

Geng *et al. Satell Navig*   (2021) 2:17

Page 5 of 15

Table 2 Details of different phase bias products and formats

Items	Strategies	Product formats
WUM	System: GPS/Galileo/BDS-2/BDS-3 Signals: C1W/C2W/L1C/L2W (G) C1C/C5Q/L1C/L5Q (E) C2I/C6I/L2I/L6I (C) Antenna: igs14.atx	Clock: Phase clock Phase bias: Bias-SINEX format V1.00
COM	System: GPS/Galileo Signals: C1C/C1W/C2C/C2W/ L1C/L1W/L2C/L2W/L2X (G) C1C/C5Q/ L1C/L1X/L5Q/L5X (E) Antenna: M14.atx	Clock: Phase clock Phase bias: Bias-SINEX format V1.00
GRG	System: GPS/Galileo Signals: C1/C2/L1/L2 (G) C1/C5/L1/L5 (E) Antenna: igs14.atx	Clock: Integer clock Phase bias: Wide-lane fractional-cycle bias
GRG-gbm	System: GPS/Galileo/BDS-2 Signals: C1C/C1W/C2W/L1C/L2W (G) C1X/C5X/L1X/L5X (E) C2I/C7I/L2I/L7I (C) Antenna: igs14.atx	Clock: GBM clock Phase bias: Bias-SINEX format V1.00
SGG-com	System: GPS/Galileo/BDS-2/QZSS Signals: C1/C2/L1/L2 (G) C1/C5/L1/L5 (E) C2/C7/L2/L7 (C) C1/C2/L1/L2 (J) Antenna: igs14.atx for GE and ESA estimates for BDS-2	Clock: COM clock Phase bias: Wide-lane and narrow-lane fractional-cycle bias
SGG-grg	System: GPS/Galileo Signals: C1/C2/L1/L2 (G) C1/C5/L1/L5 (E) Antenna: igs14.atx	Clock: GRG clock Phase bias: Wide-lane and narrow-lane fractional-cycle bias
SGG-gbm	System: GPS/Galileo/BDS-2/QZSS Signals: C1/C2/L1/L2 (G) C1/C5/L1/L5 (E) C2/C7/L2/L7 (C) C1/C2/L1/L2 (J) Antenna: igs14.atx for GE and ESA estimates for BDS-2	Clock: GBM clock Phase bias: Wide-lane and narrow-lane fractional-cycle bias

frequencies. However, in all other cases of wide-lane phase bias products in Table 2, Eq. (4) is banned because those products are based on the Melbourne-Wübbena combination observables without antenna phase center corrections.
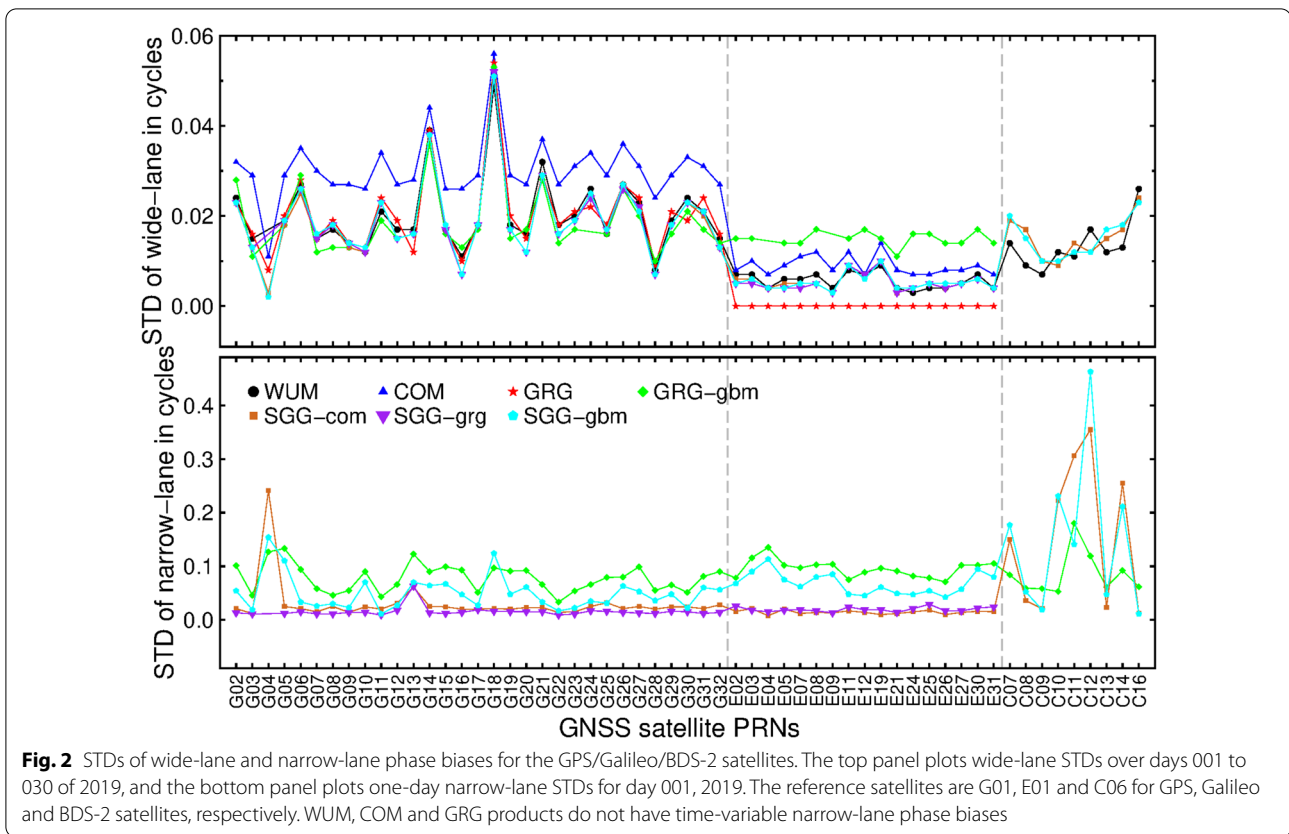
Results

Quality of phase bias products

At first, the time series of one-month wide-lane phase biases are analyzed to evaluate their temporal stability. The mean Standard Deviation (STD) for each satellite pair over the 30 days of 2019 is calculated, which are shown in Fig. 2. Note that GRG's Galileo wide-lane phase biases are constants over the 30 days and thus their STDs are zero. We can see that the STDs of GPS satellites generally show good consistency with each other. Among all GPS satellites, G18 has the largest STD of about 0.06 cycles, but most STDs are less than 0.03 cycles. SGG-com, SGG-grg and SGG-gbm share very similar STDs.

Overall, Galileo satellites have the most stable wide-lane phase biases and the mean STD is as small as 0.01 cycles. BDS satellites show a mean STD of about 0.02 cycles for their wide-lane phase biases, while the GPS STDs are usually larger than their Galileo and BDS counterparts. These results confirm that wide-lane phase biases are quite stable over time.

In the bottom panel of Fig. 2, the mean STDs of narrow-lane phase biases are plotted for all GPS, Galileo and BDS-2 IGSO/MEO (Inclined Geosynchronous Satellite Orbit/Medium Earth Orbit) satellites. Specifically, C06, C07, C08, C09, C10, C13 and C16 are IGSO satellites, and C11, C12 and C14 are MEO satellites. Since COM, WUM provide daily narrow-lane phase bias products and GRG uses integer clocks, we only present the STDs of the 15-min narrow-lane phase biases by SGG and GRG-gbm for day 001 of 2019. As shown in Fig. 2, for all GPS and Galileo satellites, the narrow-lane STDs for SGG-com and SGG-grg are clearly smaller than those for SGG-gbm

Fig. 2 STDs of wide-lane and narrow-lane phase biases for the GPS/Galileo/BDS-2 satellites. The top panel plots wide-lane STDs over days 001 to 030 of 2019, and the bottom panel plots one-day narrow-lane STDs for day 001, 2019. The reference satellites are G01, E01 and C06 for GPS, Galileo and BDS-2 satellites, respectively. WUM, COM and GRG products do not have time-variable narrow-lane phase biases

and GRG-gbm. In particular, while the narrow-lane STDs from SGG-com and SGG-grg are below 0.03 cycles, the STDs for SGG-gbm and GRG-gbm are usually larger than 0.05 cycles. In contrast, the STDs of BDS-2 narrow-lane phase biases show the largest variations from satellite to satellite, no matter whether they are from GRG-gbm, SGG-com or SGG-gbm. Compared to BDS IGSOs, BDS MEOs have relatively larger STDs. One explanation is that the number of stations that observe a BDS MEO satellite at the same time outside Asia-Oceania can be as low as four, which often leads to a poorer precision of MEO narrow-lane phase biases.

Phase biases are used to correct float ambiguities to recover their integer nature. We hence analyze the residuals of float ambiguities after phase bias corrections to further investigate the precision of all sorts of phase bias products in Table 2. Note that float ambiguities are calculated using daily ambiguity-float PPP. Figures 3 and 4 then show the distribution of the wide-lane and narrow-lane ambiguity residuals after phase bias corrections, respectively. In Fig. 3, the STDs of GPS wide-lane ambiguity residuals are 0.09 cycles for all phase bias products, and about 72% of all residuals fall in ±0.1 cycles, suggesting the similar performance of all organizations' wide-lane phase biases. In the case of Galileo, more than

80% of wide-lane ambiguity residuals fall in ±0.1 cycles for all products and their STDs are about 0.07 cycles. It is worth mentioning that, in the case of the GRG-gbm Galileo phase biases, only 60% of wide-lane ambiguity residuals will be within ±0.1 cycles and the STD will be increased to 0.1 cycles if the antenna phase center corrections are not applied to the Melbourne-Wübbena combinations, as demonstrated in Eqs. (3) and (4). While GPS and Galileo wide-lane phase bias products can overall achieve outstanding performance in recovering the integer property of wide-lane ambiguities, BDS products perform clearly worse, as shown in the rightmost panels of Fig. 3. Usually less than 50% of BDS-2 wide-lane residuals are within ±0.1 cycles, no matter which signal combination (i.e., B1I/B2I or B1I/B3I) is used. The STDs of all BDS-2 ambiguity residuals reach up to 0.2 cycles, more than doubling those for GPS and Galileo. The SGG-com and SGG-gbm based wide-lane ambiguity residuals seem to be biased by about 0.05 cycles as their peak distributions are not close to zero. Conversely, BDS-3 wide-lane phase bias products from WUM can achieve comparable performance with that of GPS, i.e., over 76% of ambiguity residuals fall in ±0.1 cycles.

GPS narrow-lane ambiguity residuals appear much better than their wide-lane counterparts in terms of
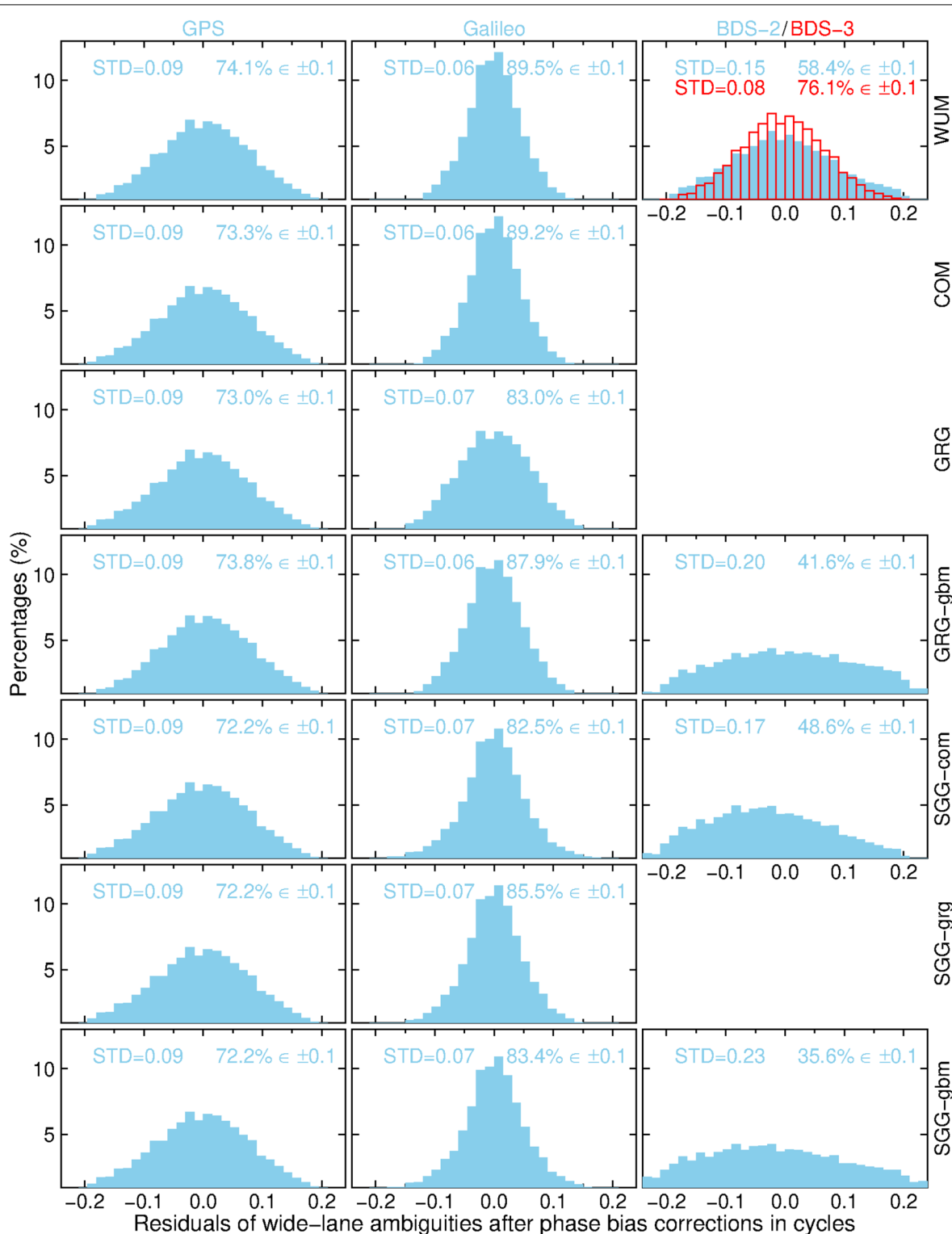
Fig. 3 Distribution of GPS, Galileo and BDS wide-lane ambiguity residuals after phase bias correction from WUM, COM, GRG, GRG-gbm, SGG-com, SGG-grg and SGG-gbm products over the 30 days of 2019. The STDs of all residuals and the percentages of all within ± 0.1 cycles are plotted at the top left and top right corners of each panel, respectively. Note that only WUM has BDS-3 products which are denoted with red open bars; WUM BDS-2 products are based on B1I/B3I signals while all other BDS-2 products are based on B1I/B2I signals

Geng *et al. Satell Navig*   (2021) 2:17

Page 8 of 15
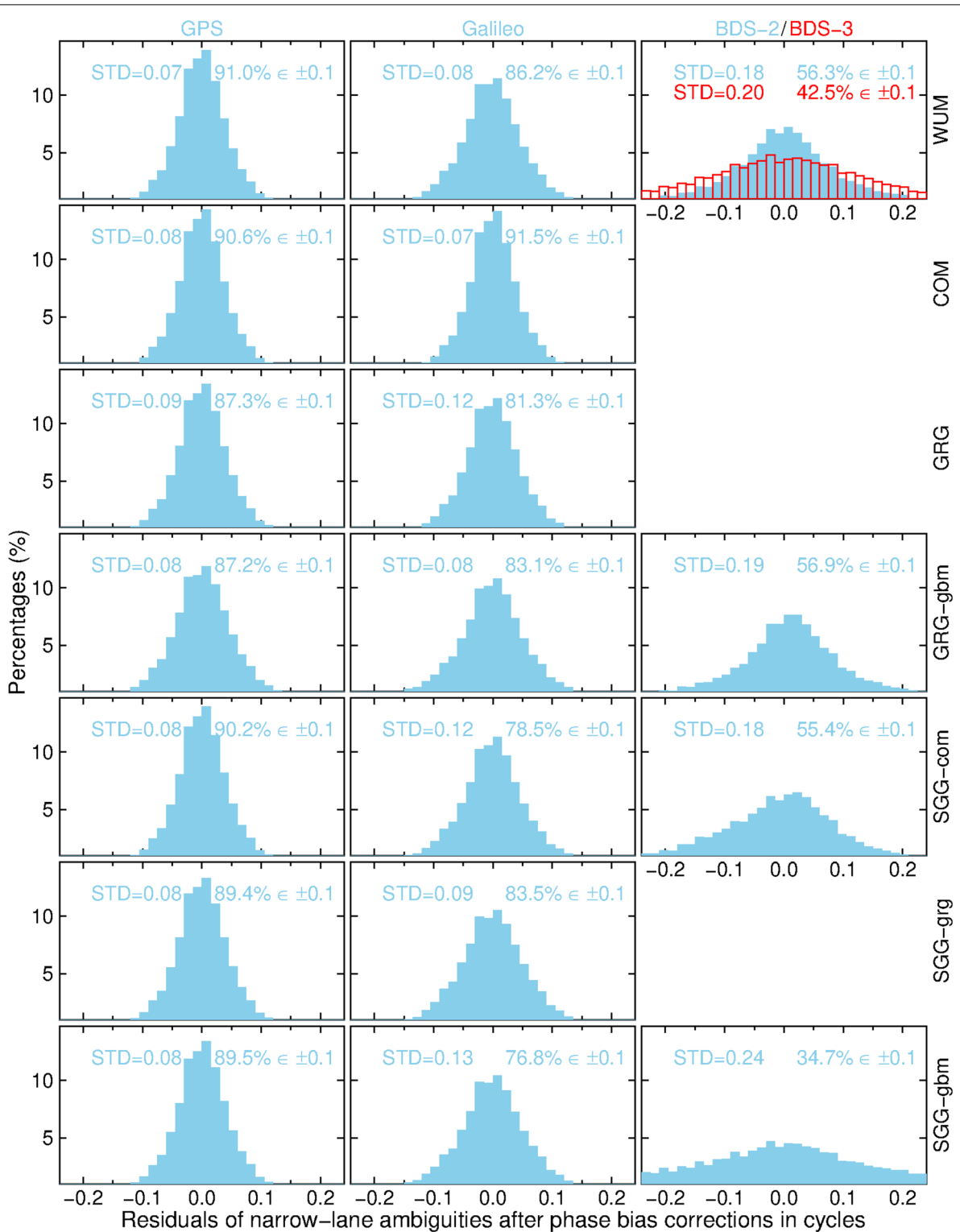
Fig. 4 Distribution of narrow-lane ambiguity residuals after phase bias corrections over the 30 days of 2019. Refer to Fig. 3 for more explanations on the symbols
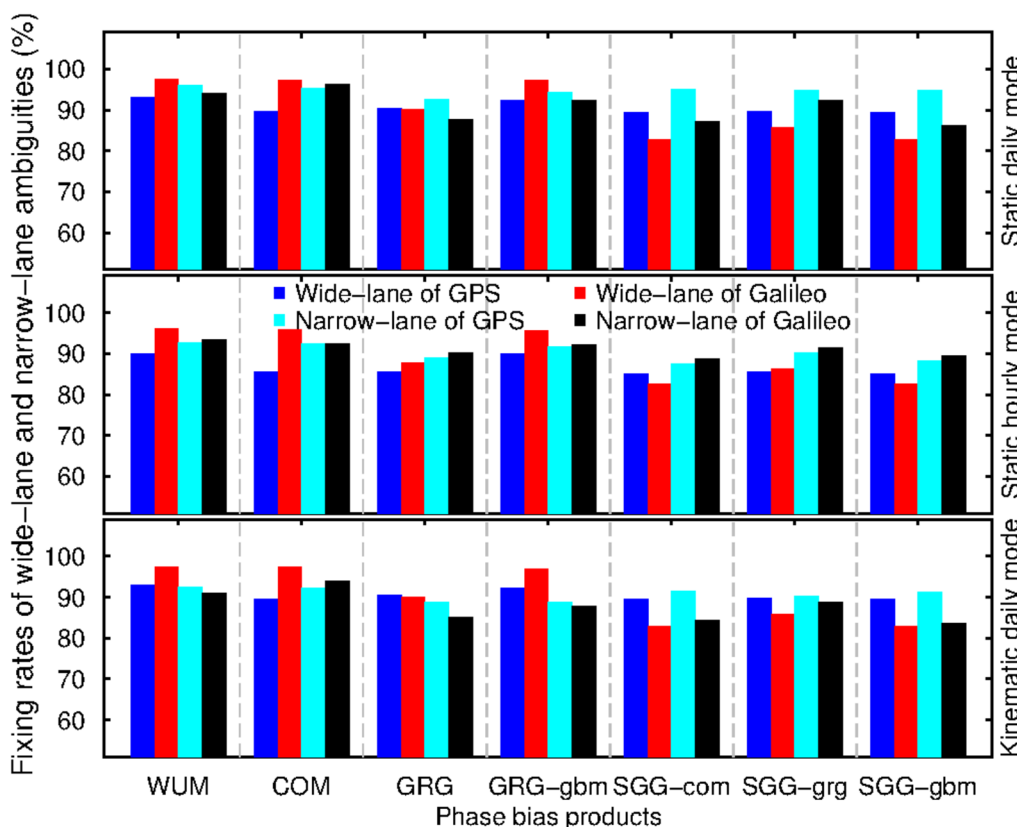
Fig. 5 Average wide-lane and narrow-lane ambiguity fixing rates for GPS/Galileo PPP-AR based on WUM, COM, GRG, GRG-gbm, SGG-com, SGG-grg and SGG-gbm phase bias products

the distribution, as shown in Fig. 4. The GPS narrow-lane ambiguity residuals for all products have STDs of less than 0.1 cycles and more than 87% of residuals are within ± 0.1 cycles. Similarly, Galileo narrow-lane phase bias products from all organizations perform comparably, although WUM and COM products have higher percentages (> 85%) of narrow-lane ambiguity residuals falling in ± 0.1 cycles. In the case of BDS-2 narrow-lane phase bias products, about 55% of narrow-lane ambiguity residuals for the WUM, GRG-gbm and SGG-com products are within ± 0.1 cycles, but the SGG-gbm products can only make about 30% of ambiguity residuals fall in ± 0.1 cycles. The STDs of all BDS-2 narrow-lane ambiguity residuals are about 0.2 cycles, almost doubling those of GPS and Galileo. Moreover, WUM BDS-3 products perform worse than their BDS-2 counterparts as only 42% of residuals fall in ± 0.1 cycles. Overall, we demonstrate that the GPS/Galileo phase bias products have the best performance in recovering integer PPP ambiguities, while the BDS products perform inferiorly. One plausible cause is that BDS observations and orbits/clocks are not as good as those of GPS and Galileo over the test period in this study.

GPS/Galileo PPP-AR
Daily solutions
In this section, we carry out static PPP-AR using 24 h of GPS/Galileo data. Ambiguity fixing is achieved through the bias fixing method proposed by Dong and Bock (1989). A seven-parameter Helmert transformation is applied before calculating the position RMS error of our PPP solutions against the IGS weekly solutions. Note that a threshold of five times the RMS error is used to remove outlier solutions, and finally about 1% of all solutions are removed.

The top panel of Fig. 5 shows the average ambiguity fixing rates at all stations over the 30 days. WUM shows the highest GPS fixing rates of 93.0% and 96.1% for the wide-lane and narrow-lane ambiguities, respectively. Though WUM's Galileo fixing rates (i.e., 97.4% and 94.0%) are even higher than its GPS fixing rates, the COM phase products achieve overall the highest among all products, which are 97.3% and 96.4%. Different from WUM, COM and GRG-gbm, the Galileo wide-lane ambiguity fixing rates of all SGG phase bias products are lower than those of GPS. Again, we note that the Galileo wide-lane ambiguity fixing rates will decline to 68% if the antenna phase

Geng *et al. Satell Navig*   (2021) 2:17

Page 10 of 15

Table 3 Mean position RMS errors of GPS/Galileo daily PPP-AR of days 001 to 030, 2019

Product names	Float solutions in different directions (mm)	Fixed (mm)	Improvement
	E/N/U	E/N/U	(%)
WUM	3.3/2.1/6.4	2.0/2.0/5.9	39.4/4.8/7.8
COM	3.0/2.1/6.6	1.9/2.1/6.1	36.7/0.0/7.6
GRG	3.3/2.1/6.4	2.1/2.0/6.0	36.4/4.8/6.3
GRG-gbm	3.7/2.8/7.5	2.5/2.7/7.0	32.4/3.6/6.7
SGG-com	3.1/2.1/6.7	1.9/2.1/6.3	38.7/0.0/6.0
SGG-grg	3.3/2.2/6.5	2.0/2.1/6.0	39.4/9.1/7.7
SGG-gbm	3.2/2.2/6.4	2.2/2.1/6.0	31.2/9.1/6.3

center errors are ignored in the Melbourne-Wübbena combinations (see Eq. 3). In addition, we find that the GPS fixing rates for the SGG-com products are comparable with those based on COM. However, for the Galileo satellites, the wide-lane and narrow-lane ambiguity fixing rates for SGG-com are 10%-15% point lower compared to COM. This phenomenon may be caused by the igs14.atx antenna corrections used by SGG-com, which however differ from M14.atx adopted by COM Galileo orbit/clock products.

Table 3 shows the mean position RMS errors over all stations for the 30 days. The WUM ambiguity-fixed position RMS errors are 2.0, 2.0, and 5.9 mm in the east, north and up components, respectively, while those of float solutions are 3.3, 2.1, and 6.4 mm, showing a pronounced improvement of 39% in the east. In fact, all phase bias products can lead to such improvement of over 30% while the north and up components show modest improvements of less than 10%, as exhibited by the last column of Table 3. Moreover, both GRG-gbm and SGG-gbm show the most inferior improvements (i.e., less than 33%) for the east component compared to other phase bias products. We note that the GBM satellite clocks, as used by GRG-gbm and SGG-gbm, are estimated without fixing undifferenced ambiguities, while all other phase bias products use ambiguity-fixed satellite clocks. This point may explain why GRG-gbm and SGG-gbm have inferior position RMS errors against the IGS weekly solutions (Geng et al., 2019a).
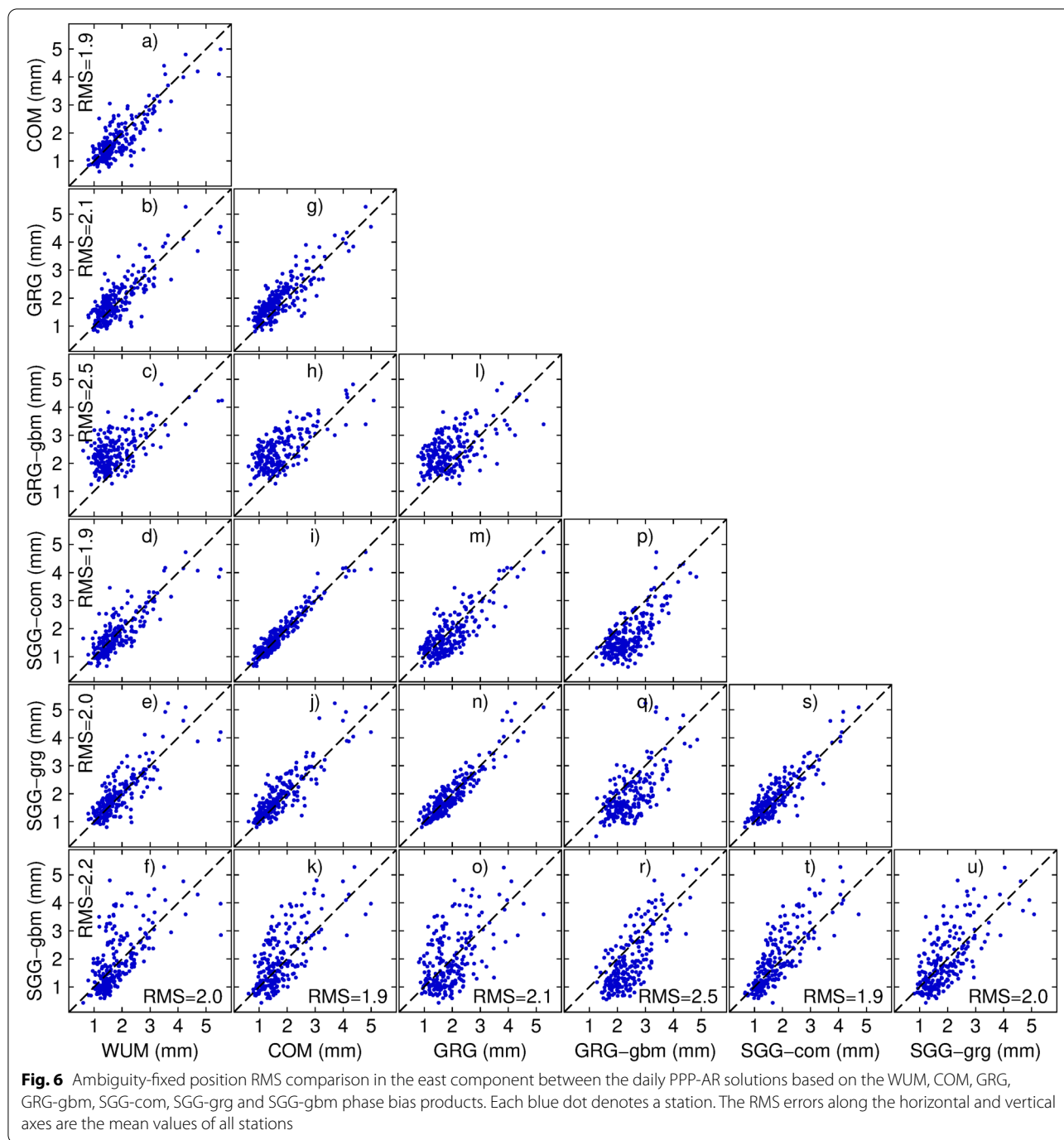
In order to investigate the daily positioning performance based on various phase bias products, Fig. 6 compares the ambiguity-fixed position RMS errors at all 300 stations for the east component. Within a panel, if a blue dot is located above the dashed diagonal line, its position RMS error corresponding to the horizontal axis will be smaller than that corresponding to the vertical axis; the more dots located above the diagonal line, the better the

solutions corresponding to the horizontal axis. In this manner, we can clearly see that GRG-gbm performs the worst among all phase bias products (see panels c, h, i, p, q and r). This is also the case for the north and up components (not shown here though), thus echoing the statistics in Table 3. Similarly, SGG-gbm seems to have clearly more stations with position RMS of over 3 mm, compared to WUM, COM, GRG and SGG-com (see panels f, k, o, t and u), thereby showing its slightly worse daily positioning performance. In addition, SGG-com and SGG-grg can achieve very similar position RMS errors to those of COM and GRG, respectively (see panels i and n). We point out that SGG-com and SGG-grg phase bias products take advantages of COM and GRG's phase/integer clock products in the computation of the 15-min UPDs. Overall, we demonstrate that all phase bias products can be used for high-precision GPS/Galileo PPP-AR with daily data.

Static hourly solutions
This section investigates GPS/Galileo static PPP-AR based on hourly data. Unlike the daily solutions where float narrow-lane ambiguities are fixed directly using the bootstrapping strategy (Dong & Bock, 1989), the LAMBDA (least-squares ambiguity decorrelation) method is used to search for integer ambiguities in hourly solutions (Teunissen, 1995). We remove those solutions of which any coordinate component has an error of larger than 5 cm or five times the RMS error. As a consequence, 6%-8% of all solutions are removed for each phase bias product. The ambiguity fixing rates are shown in the middle panel of Fig. 5. We can find that Galileo narrow-lane ambiguity fixing rates are higher than those of GPS for all phase bias products. Generally, Galileo fixing efficiency is higher than that of GPS. The Galileo wide-lane ambiguity fixing rates of SGG-gbm and SGG-com are slightly lower than those of GPS.

Table 4 shows the mean position RMS errors and the improvement rates. We can find that hourly solutions show significant improvements in both east and north components once PPP-AR is achieved. Again, COM-based solutions achieve the highest positioning precision among all phase bias products; the mean position RMS error is reduced from 7.3, 5.9, and 12.7 mm in the ambiguity-float solutions to 3.8, 3.7, and 11.4 mm in the ambiguity-fixed solutions for the east, north and up components, respectively. WUM, GRG, SGG-com and SGG-grg achieve comparable positioning precisions. However, the mean position RMS errors of GRG-gbm and SGG-gbm PPP-AR are 4.7, 4.5, 12.8, 4.4, 4.3, and 12.3 mm in east (E), north (N) and up (U) components, respectively, which are worse than those based on other phase bias

Fig. 6 Ambiguity-fixed position RMS comparison in the east component between the daily PPP-AR solutions based on the WUM, COM, GRG, GRG-gbm, SGG-com, SGG-grg and SGG-gbm phase bias products. Each blue dot denotes a station. The RMS errors along the horizontal and vertical axes are the mean values of all stations

products. These results echo those in Table 3 for daily solutions.

Kinematic solutions

In this section, we implement kinematic PPP-AR using 24 h of GPS/Galileo data. PPP ambiguities are resolved using the bias fixing method developed by Dong and Bock (1989). At each station, we remove the epochs

with less than four satellites, and those where any coordinate component has an error of larger than 10 cm or five times the RMS error. Generally, less than 2% of solutions are removed, but GRG-gbm has over 3% of solutions eliminated. From the bottom panel of Fig. 5, we can see that the Galileo wide-lane ambiguity fixing rates are higher than those of GPS for the WUM and COM phase bias products; in contrast, the SGG phase bias products

Geng *et al. Satell Navig*   (2021) 2:17

Page 12 of 15

Table 4 Mean position RMS errors of hourly GPS/Galileo PPP-AR for day 001 to 030 of 2019

Product names	Float solutions in different directions (mm)	Fixed (mm)	Improvement (%)
	E/N/U	E/N/U	E/N/U
WUM	7.4/6.0/13.1	4.1/4.0/11.9	44.6/33.3/9.2
COM	7.3/5.9/12.7	3.8/3.7/11.4	47.9/37.3/10.2
GRG	7.4/6.1/12.8	4.1/4.0/11.8	44.6/34.4/7.8
GRG-gbm	7.4/6.0/13.6	4.7/4.5/12.8	36.5/25.0/5.9
SGG-com	7.4/6.0/12.9	4.3/4.0/12.1	41.9/33.3/6.2
SGG-grg	7.4/6.2/12.9	4.2/4.0/12.2	43.2/35.5/5.4
SGG-gbm	7.4/5.8/12.7	4.4/4.3/12.3	40.5/25.9/3.1

Table 5 Mean position RMS errors of kinematic GPS/Galileo PPP-AR for day 001 to 030 of 2019

Product names	Float solutions in different directions (mm)	Fixed (mm)	Improvement (%)
	E/N/U	E/N/U	E/N/U
WUM	9.3/9.1/22.3	7.0/8.4/20.9	24.7/7.7/6.3
COM	8.7/7.8/21.6	6.6/7.1/20.0	24.1/9.0/7.4
GRG	9.6/8.5/22.6	7.0/7.8/21.5	27.1/8.2/4.9
GRG-gbm	10.2/9.0/23.9	7.8/8.2/22.9	23.5/8.9/4.2
SGG-com	8.9/8.0/22.3	6.8/7.3/21.3	23.6/8.8/4.5
SGG-grg	9.8/8.6/23.2	7.2/7.9/21.7	26.5/8.1/6.5
SGG-gbm	8.9/8.2/22.3	7.0/7.5/21.5	21.3/8.5/3.6

show the opposite. Regarding the narrow-lane ambiguity fixing rates, the SGG-gbm and SGG-com products also perform worse compared to others.

As shown in Table 5, after PPP-AR, COM phase bias products manifest the best performance by improving the position RMS errors from 8.7, 7.8, and 21.6 mm to 6.6, 7.1, and 20.0 mm in the east, north and up components, suggesting improvement rates of 24.1%, 9.0% and

7.4%, respectively. All other products except GRG-gbm seem to perform comparably for all three coordinate components. In particular, GRG-gbm can only achieve a position RMS error of 7.8 mm for the east component, which is 18% worse than that of COM and echo again the results in Tables 3 and 4.

BDS-only PPP-AR

At the moment of this study, only WUM, GRG-gbm and SGG provide BDS phase bias products for the IGSO and MEO satellites. GEO (Geosynchronous Earth Orbit) satellites are all excluded in the study. We select 34 IGS BDS-2/BDS-3 stations in Asia spanning days 244 to 273 of 2019 to implement BDS-only PPP-AR (Fig. 1). Since the SGG products are not regularly released, this period of 30 days is chosen as the WUM, GRG-gbm and SGG-gbm products all have BDS phase biases except for SGG-com. It is worth noting that the BDS-3 data after the first half of 2020 will be much better to enable PPP-AR since more satellites are available. Therefore, we also tested the BDS data for days 244–273 of 2020 using the WUM BDS phase biases. Note that the WUM products include both BDS-2 (B1I/B3I) and BDS-3 (B1I/B3I) phase biases, while GRG-gbm and SGG-gbm support BDS-2 (B1I/B2I) only. BDS-2 satellites' nadir-dependent pseudorange biases are corrected before PPP-AR (Wanninger & Beer, 2014). Outlier solutions are removed if they exceed five times the position RMS errors. Since there are usually no enough BDS satellites to be observed at a station in 2019, up to 15%-22% of all solutions are removed. In contrast, 8%-10% of BDS solutions were removed for the year of 2020.

Table 6 shows that the mean position RMS error of BDS-only daily PPP-AR is not as good as that of GPS/Galileo (Table 3). The RMS errors of WUM ambiguity-float PPP for 2019 are only 10.8, 8.4, and 32.4 mm in the east, north and up components, respectively, and those of the ambiguity-fixed PPP are 10.1, 8.1, and 32.2 mm. No coordinate component shows a significant improvement,

Table 6 Mean position RMS error of BDS-only daily PPP-AR for days 244 to 273 of 2019 and 2020

Product names		Mean number of satellites	Float solutions in different directions (mm)	Fixed (mm)	Fixing rates (%)	
			E/N/U	E/N/U	Wide-lane	Narrow-lane
WUM (2019)	BDS-2	5	10.8/8.4/32.4	10.1/8.1/32.2	90.44	81.22
GRG-gbm	BDS-2	5	13.5/10.9/25.9	11.8/9.8/25.8	54.54	77.14
SGG-gbm	BDS-2	5	12.7/7.6/26.9	9.9/7.4/26.3	76.40	77.26
WUM (2019)	BDS-2/ BDS-3	8	8.9/6.8/21.9	7.3/6.7/22.5	92.44	73.11
WUM (2019)	BDS-3	3	17.7/10.5/23.7	14.9/10.4/25.0	95.59	48.08
WUM (2020)	BDS-2/ BDS-3	10	9.2/5.4/15.1	6.2/5.3/16.0	92.22	68.41
WUM (2020)	BDS-3	5	11.8/5.7/17.5	8.6/5.6/19.2	95.70	61.02
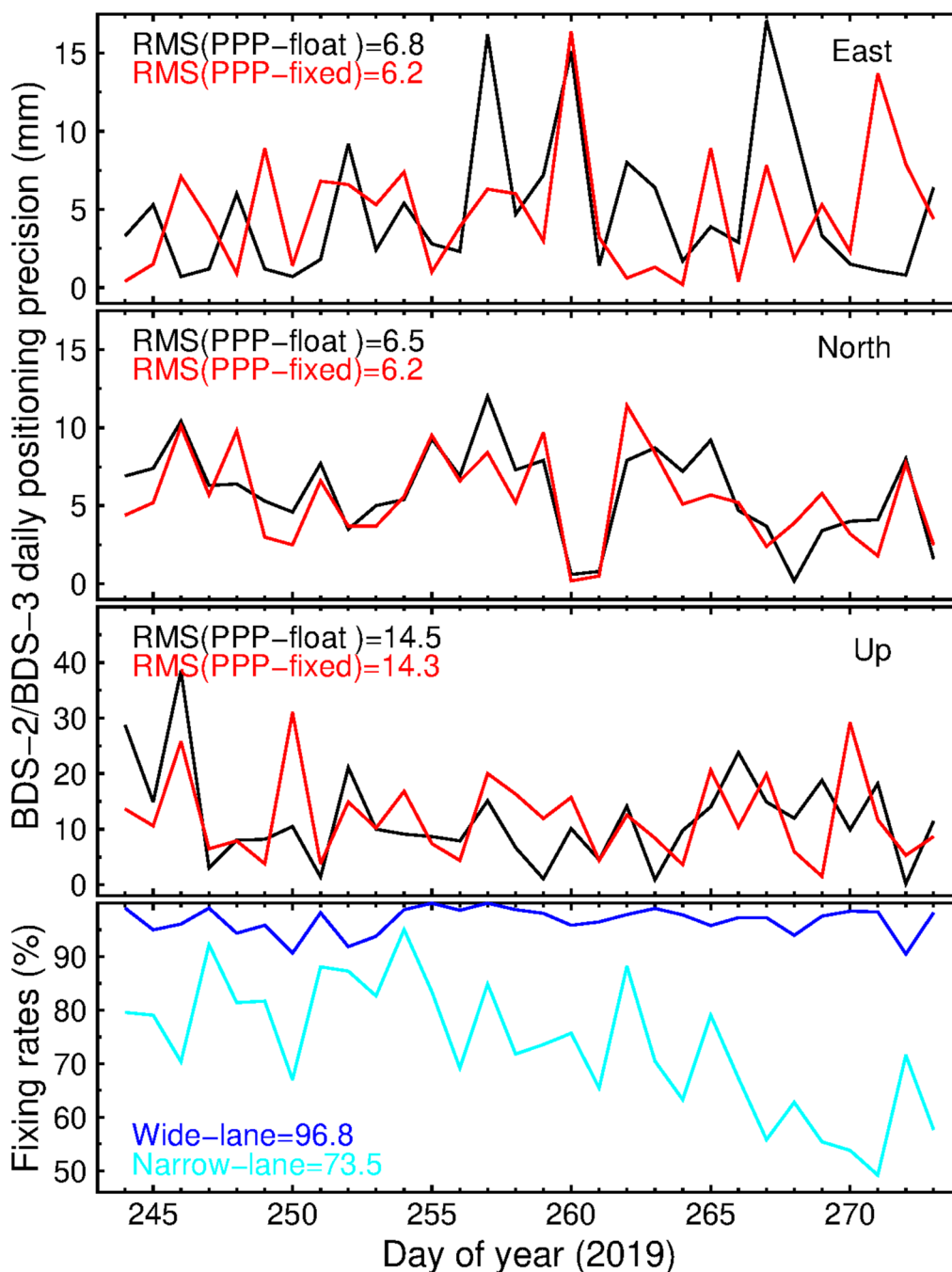
Fig. 7 BDS-2/BDS-3 positioning precision and ambiguity fixing rates at station SOLO in 2019 using the WUM phase bias products (see Fig. 1 for the location of SOLO)

although the fixing rates of BDS-2 wide-lane and narrow-lane ambiguities reach 90% and 81%, respectively. Similarly, GRG-gbm and SGG-gbm show slight improvements in terms of the mean position RMS errors, though the narrow-lane ambiguity fixing rates can reach 77%. One explanation for such inferior BDS-2 positioning

precisions is that, most of the time, BDS-2 PPP-AR might be unreliable due largely to the insufficient number of BDS satellites over the year of 2019 (Column 3 in Table 6). The ambiguity fixing rates cannot be taken as a diagnostic of the achievable positioning precision. A typical example is Fig. 7 where the ambiguity-fixed

Geng *et al. Satell Navig*   (2021) 2:17

Page 14 of 15

positioning precision is not always better than the ambiguity-float precision for the year of 2019, even though the ambiguity fixing rates might look decent.

Furthermore, we integrate BDS-2 and BDS-3 observations for PPP-AR using the WUM products in both 2019 and 2020. The mean position RMS errors of WUM ambiguity-float PPP for 2019 are 8.9, 6.8, and 21.9 mm in the east, north and up components, respectively, while those of ambiguity-fixed PPP are 7.3, 6.7, and 22.5 mm. BDS-2/BDS-3 PPP-AR shows minor (18%) positioning precision improvement in contrast to its ambiguity-float counterpart. When more BDS satellites are visible for the year of 2020, ambiguity-fixed BDS-2/BDS-3 PPP shows 33% improvement compared to ambiguity-float PPP in terms of the east positioning precision. The east positioning precision of BDS-3 PPP-AR is about 50% worse than BDS-2 PPP-AR for the year of 2019 since only three BDS-3 satellites are visible for each epoch on average. This situation is reversed in 2020 where the BDS-3 PPP-AR achieves better positioning precision than BDS-2 PPP-AR for all three coordinate components. Moreover, WUM BDS-2/BDS-3 shows lower narrow-lane ambiguity fixing rate of around 70% compared to 81% of BDS-2. We therefore carry out BDS-3 only PPP-AR and find that its narrow-lane ambiguity fixing rate is as low as 48% in 2019 and 60% in 2020, echoing the distribution statistics of BDS-3 narrow-lane ambiguity residuals in Fig. 4.

The causes for the poor positioning precision of BDS-only PPP-AR in 2019 are twofold. On the one hand, the relatively poor BDS orbits and the imprecise error models (e.g., solar radiation pressure, satellite attitudes, etc.) limit the positioning precision of BDS-only PPP. On the other hand, BDS phase bias products cannot be computed precisely since the number of usable BDS stations is not always enough, and the number of BDS satellites observed by a station is not enough either, during the test periods of this study.

Conclusions
In this study, we carry out PPP-AR at 300 globally-distributed stations using seven sorts of phase bias products. Generally, all GPS/Galileo phase biases from WUM, COM, GRG and SGG can enable static and kinematic PPP-AR in an efficient manner.

For the GPS/Galileo daily solutions, all phase bias products are able to improve the positioning precision for the east component by more than 30% after ambiguity fixing. In particular, the phase bias products based on GBM satellite orbits and clocks (i.e., GRG-gbm and SGG-gbm) deliver the lowest improvement rates after PPP-AR. In the case of hourly static GPS/Galileo solutions, both east and north components can have more than 30% improvement in terms of positioning precisions, while

again the GRG-gbm and SGG-gbm products show inferior performance compared to others.

In the case of BDS-2 or BDS-3 only daily solutions, insufficient satellite number (5 for BDS-2 and 3 for BDS-3 on average observed by an Asia-Oceania station) limits the performance of PPP-AR using the BDS-2/BDS-3 phase bias products from WUM, GRG-gbm and SGG-gbm in the year of 2019. We argue that BDS-2/BDS-3 PPP-AR was unreliable even though a decent fixing rate might be achieved over the year of 2019. Fortunately, the BDS-3 constellation has been fully operational since July 31, 2020, and BDS-2/BDS-3 phase biases are more reliable and precise to enable PPP-AR where the horizontal coordinate components can achieve about 5 mm precision.

References
Banville, S., Geng, J., Loyer, S., Schaer, S., Springer, T., & Strasser, S. (2020). On the interoperability of IGS products for precise point positioning with ambiguity resolution. *Journal of Geodesy, 94*(1), 10

Boehm, J., Niell, A. E., Tregoning, P., & Schuh, H. (2006). Global mapping function (GMF): A new empirical mapping function based on numerical weather model data. *Geophysical Research Letters, 25*(33), L07304

Collins, P., Bisnath, S., Lahaye, F., & Héroux, P. (2010). Undifferenced GPS ambiguity resolution using the decoupled clock model and ambiguity datum fixing. *Navigation, 57*(2), 123–135

Dilssner, F., Springer, T., Schönemann, E. & Enderle, W. (2014). Estimation of satellite antenna phase center corrections for BeiDou. In: *IGS Workshop 2014*, Pasadena, CA, USA, Jun. 23–27

Dong, D., & Bock, Y. (1989). Global positioning system network analysis with phase ambiguity resolution applied to crustal deformation studies in California. *Journal of Geophysical Research, 94*(B4), 3949–3966

Fritsche, M., Dietrich, R., Knöfel, C., Rülke, A., Vey, S., Rothacher, M., & Steigenberger, P. (2005). Impact of higher-order ionospheric terms on GPS estimates. *Geophysical Research Letters, 32*(23), L23311

Gabor, M. J. & Nerem, R. S. (1999). GPS carrier phase ambiguity resolution using satellite-satellite single differences. In: *Proceedings of the 12th International Technical Meeting of the Satellite Division of the Institute of Navigation (ION GPS 1999),* 14–17 Sept., Nashville, TN, USA. pp. 1569–1578

Ge, M., Gendt, G., Rothacher, M., Shi, C., & Liu, J. (2008). Resolution of GPS carrier-phase ambiguities in precise point positioning (PPP) with daily observations. *Journal of Geodesy, 82*(7), 389–399

Geng, J., Chen, X., Pan, Y., Mao, S., Li, C., Zhou, J., & Zhang, K. (2019b). PRIDE PPP-AR: an open-source software for GPS PPP ambiguity resolution. *GPS Solut, 23*, 91. https://doi.org/10.1007/s10291-019-0888-1

Geng, J., Chen, X., Pan, Y., & Zhao, Q. (2019a). A modified phase clock/bias model to improve PPP ambiguity resolution at Wuhan University. *Journal of Geodesy, 93*(10), 2053–2067

Geng, J., Teferle, F. N., Shi, C., Meng, X., Dodson, A. H., & Liu, J. (2009). Ambiguity resolution in precise point positioning with hourly data. *GPS Solutions, 13*(4), 263–270

Ghoddousi-Fard, R., & Dare, P. (2006). Online GPS processing services: an initial study. *GPS Solutions, 10*(1), 12–20

Guo, J., Xu, X., Zhao, Q., & Liu, J. (2015). Precise orbit determination for quad-constellation satellites at Wuhan University: strategy, result validation, and comparison. *Journal of Geodesy, 90*(2), 143–159

Hofmann-Wellenhof, B., Lichtenegger, H., & Collins, J. (2001). *Global Positioning System*. Springer

Hu, J., Zhang, X., Li, P., Ma, F., & Pan, L. (2020). Multi-GNSS fractional cycle bias products generation for GNSS ambiguity-fixed PPP at Wuhan University. *GPS Solutions, 24*(1), 1–13

Kouba, J., & Héroux, P. (2001). Precise point positioning using IGS orbit and clock products. *GPS Solutions, 5*(2), 12–28

Laurichesse, D., (2011). The CNES Real-time PPP with undifferenced integer ambiguity resolution demonstrator, In: *Proceedings of the ION GNSS 2011*, September 2011, Portland, Oregon

Laurichesse, D. (2015). Carrier-phase ambiguity resolution: Handling the biases for improved triple-frequency PPP convergence. *GPS World, 26*, 49–54

Laurichesse, D., Mercier, F., Berthias, J. P., Broca, P., & Cerri, L. (2009). Integer ambiguity resolution on undifferenced GPS phase measurements and its application to PPP and satellite precise orbit determination. *Navigation, 56*(2), 135–149

Melbourne, W. G. (1985). The case for ranging in GPS based geodetic systems. In: *Proceedings 1st International Symposium on Precise Positioning with the Global Positioning System*, Rock- ville, 15–19 April, MD, USA, pp. 373–386

Petit, G., & B. Luzum (2010). IERS Conventions (2010). IERS Tech. Note 36, Verlag des Bundesamts für Kartographie und Geodäsie, Frankfurt am Main, Germany

Saastamoinen, J. (1972). Contributions to the theory of atmospheric refraction. *Bulletin Gæodésique, 105*(1), 279–298

Schaer, S. (2016). SINEX-Bias-Solution independent exchange format for GNSS biases version 1.00 (draft). In: *IGS Workshop on GNSS biases, Bern, Switzerland*, 5–6.

Schaer, S., Villiger, A., Dach, R., Prange, L., Jäggi, A. & Arnold, D. (2018). New ambiguity-fixed IGS clock analysis products at CODE. In: *IGS Workshop on analysis centres and reference frames,* Oct. 29-Nov. 2, Wuhan, China

Tétreault, P., Kouba, J., Héroux, P., & Legree, P. (2005). CSRS-PPP: an internet service for GPS user access to the Canadian spatial reference frame. *Geomatica, 59*(1), 17–28

Teunissen, P. J. G. (1995). The least-squares ambiguity decorrelation adjustment: a method for fast GPS integer ambiguity estimation. *Journal of Geodesy, 70*(1–2), 65–82

Wanninger, L., & Beer, S. (2014). BeiDou satellite-induced code pseudorange variations: Diagnosis and therapy. *GPS Solutions, 19*(4), 639–648

Wübbena, G. (1985). Software developments for geodetic positioning with GPS using TI 4100 code and carrier measurements. In: *Proceedings 1st International Symposium on Precise Positioning with the Global Positioning System*, Rockville, 15–19 April, MD, USA, pp 403–412

Zumberge, J. F., Heflin, M. B., Jefferson, D. C., Watkins, M. M., & Webb, F. H. (1997). Precise point positioning for the efficient and robust analysis of GPS data from large networks. *Journal of Geophysical Research: Solid Earth, 102*(B3), 5005–5017

Publisher's Note